JOURNAL OF AIRCRAFT
Vol. 44, No. 5, September–October 2007

Development and Testing of the *Mentor* Flapping-Wing Micro Air Vehicle

Patrick Zdunich,* Derek Bilyk,* Marc MacMaster,* and David Loewen*
Advanced Subsonics Inc., Vaughan, Ontario L4K 1X5, Canada
James DeLaurier†
University of Toronto Institute for Aerospace Studies, Toronto, Ontario M3H 5T6, Canada
and
Roy Kornbluh,‡ Tom Low,§ Scott Stanford,¶ and Dennis Holeman**
SRI International, Menlo Park, California 94025

DOI: 10.2514/1.28463

In 1997 the Defense Advanced Research Projects Agency initiated a program to explore the possibility of micro air vehicles for the purpose of individually portable surveillance systems for close-range operations. The various contractors approached the problem in several ways, such as developing tiny fixed-wing airplanes, rotary-wing aircraft, and ornithopters mimicking animal flight. This paper describes one such flapping-wing aircraft, which drew upon the clap–fling phenomenon that is exploited by many flying animals and insects for lift generation. Essentially this aircraft was a mechanical simulation of hummingbird flight, though with two sets of wings to eliminate the unbalanced side-to-side flapping forces. Two flying demonstration models were built, one with an internal-combustion engine and another with an electric motor. In both cases, these incorporated a drive train to reduce the high rpm rotary shaft motion to lower-frequency oscillation for flapping. Also required was a programmable logic board for stabilization. Successful hovering flight was achieved with both models, and initial studies of transition to horizontal flight were also explored.

I. Introduction

THE purpose of this article is to describe how a flapping-wing solution was explored for micro air vehicle (MAV) applications. This work originated in response to a Defense Advanced Research Projects Agency (DARPA) initiative in 1997 for the development of tiny remotely piloted aircraft that could be used for individually portable systems, which would enable surveillance of cluttered environments or other close-range operations. The notion was that modern microelectronics, motors, and materials were just at the stage that such a flight vehicle was feasible. Moreover, even if this notion was not quite so, the MAV program would clearly identify and motivate research directions that would provide solutions.

As with all novel initiatives, many different approaches were proposed by the various teams. The majority of these were either fixed-wing or rotary-wing configurations. For example, several successful fixed-wing designs were developed and tested by AeroVironment Inc. [1]. These used very innovative microcontrol and video systems to produce tiny (6 in. span) tailless aircraft capable of providing outdoor surveillance information. Such aircraft, though, would be impractical for indoor missions because of the speed required to sustain flight. For this purpose, other teams explored rotary-wing solutions so as to provide a hovering capability. A noteworthy example of this is the ducted-rotor design by Barrett [2] (the "Coleopter") which demonstrated both hover and transition to horizontal translational flight.

A subset of the DARPA program involved three teams exploring a flapping-wing solution, which included the Mentor team. The first two years of this initiative were under DARPA's micro air vehicle program directed by DARPA program manager James McMichael; and the final two years of the project were under DARPA's micro adaptive flow control program, directed by Richard Wlezien (for 1.5 years) and Steven Walker (for the final 6 months).

The contract lead was SRI International of Menlo Park, California (hence the "Men" in Mentor) and the subcontractor was the Subsonic Aerodynamics Group at the University of Toronto (hence the "tor" in Mentor). SRI had been developing a novel artificial muscle referred to as the EPAM™†† (electroactive polymer artificial muscle), which will be further described in this article. Such a device provides work by means of an oscillating force, which lends itself naturally to the notion of actuating a set of flapping wings. Moreover, the idea of flapping wings for a MAV seemed worth exploring because this is clearly a successful solution in nature for creatures at MAV scale. Such insects and tiny birds hover and translate with ease and have extraordinary maneuverability. Further, DARPA found this appealing because of the biomimetic possibilities (the MAV might be ignored in hostile situations if it is mistaken for a bird or insect).

SRI contacted the University of Toronto group because of their ongoing research on flapping-wing flight. This was at a much larger scale than that for an MAV, involving remotely piloted and full-scale ornithopters [3,4], but the group's analytical and experimental experience with unsteady aerodynamics and aeroelastic tailoring gave a starting point for exploring flapping wings at smaller scales. However, just as the aerodynamic behavior of large birds differs greatly from that for insects or hummingbirds, likewise the aerodynamics for the Mentor differed from that for large ornithopters. For example, as described in [5], the large ornithopter's wing performs most efficiently with fully attached flow (as is usually the case for a fixed wing); and the design incorporates a traditional-looking airfoil which, when flapped, produces thrust primarily through augmented

Received 21 October 2006; revision received 20 March 2007; accepted for publication 20 March 2007.

*Principal Researcher, 193 Jardin Drive.
†Professor Emeritus, 4925 Dufferin Street. Associate Fellow AIAA.
‡Senior Research Engineer, 333 Ravenswood Avenue.
§Program Director, 333 Ravenswood Avenue.
¶Senior Research Engineer, 333 Ravenswood Avenue.
**Principal Engineer, 333 Ravenswood Avenue.

††Artificial Muscle Inc. (AMI), Menlo Park, California.

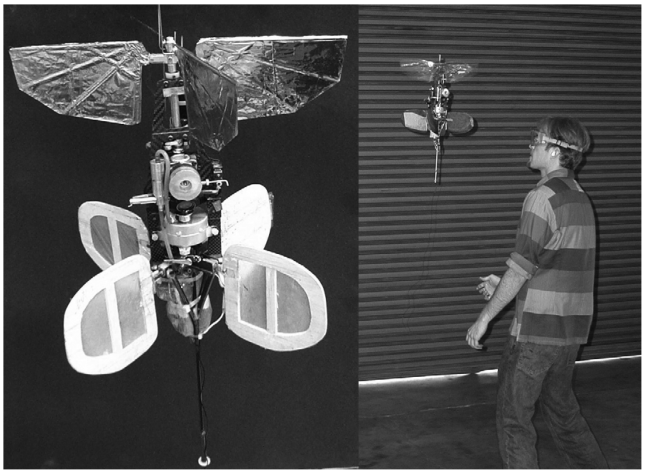

Fig. 1 Internal-combustion powered demonstration model (SF-2.5).

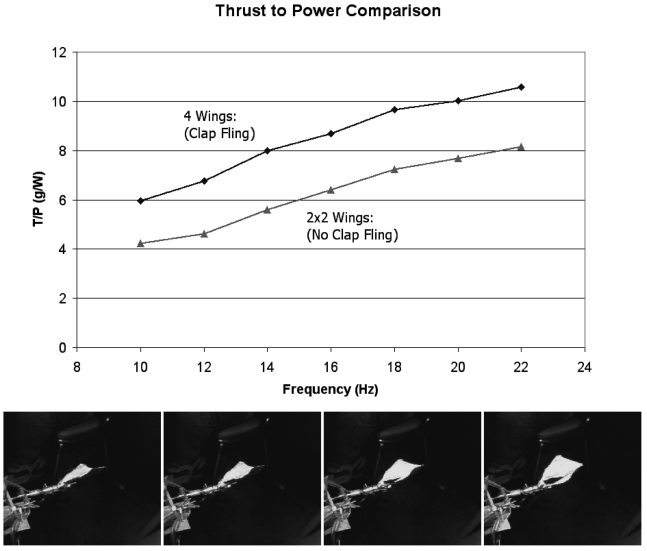

Fig. 2 Results of an experimental demonstration of the clap–fling phenomenon with a sequence of still captures of wing set on test apparatus using a strobe light.

leading-edge suction. By contrast, insect wings produce purposeful separated flow, usually taking the form of shed vortices from the leading and trailing edges.

At the time this work began, literature on this topic was limited and primarily found in zoological publications. Since then, considerable research has been performed [6–8] that has quantitatively and analytically elucidated the function of the shed vortices. In 1998, however, the primary source and inspiration for the Mentor's configuration came from the "clap–fling" hypothesis of Weis-Fogh [9], which was developed by observing the behavior of small hovering insects. It was found that they produced extraordinarily high values of average lift coefficient, which was well beyond any explanation based on attached-flow aerodynamic theories. The hypothesis, based on observation of the wings' kinematics, was that the two wing surfaces clap together and then peel apart starting at the leading edge. At the instance just before the trailing edges come apart, both wings have strong equal and opposite bound vorticity. Further, because the trailing edges were joined during this peeling action, the strength of the vorticity is much greater than that produced from Kutta condition [10] considerations. As the wings fling apart they carry this "super circulation," which thus produces a high value of lift.

For application to the Mentor, this seemed like an attractive way to produce considerable lift in a compact size (initially, the MAV was constrained to a 6 in. overall dimension). Further, to provide lateral balance, it was decided to use two pairs of clap–fling wings. This is the reasoning for the Mentor's configuration, as shown in Fig. 1. This article will describe the development of the wing design and its incorporation into a successful flying vehicle, as well as the development of the specialized drive, wing fabrication, and means for stability and control. This aircraft performed hovering flight, as well as demonstrating the potential for transition into fast horizontal flight.

II. Experimental Wing Design

As mentioned in the Introduction, the clap–fling phenomenon, which is employed by many insects and birds, was the aerodynamic principle behind the Mentor design. The hypothesis was that this significantly augments thrust for a limited actuator-disk area and provides a source of emergency performance for animal flight. It remained to verify this experimentally and demonstrate the possibility of its implementation in flapping-wing vehicles. The thrust augmentation of the clap–fling phenomenon was clearly shown by a simple experiment on an instrumented wing testing apparatus. This consisted of a strain-gage balance clamped to a lab bench, with the wings actuated by a computer-controlled servomotor driving a pair of four bar linkages. In this experiment two pairs of wings, arranged in an X configuration (as seen from the top), were shown to produce more than twice the thrust of a single pair of wings mounted opposite to one another and not clap flinging. Therefore, the clap–fling interaction of the wings clearly produces this thrust augmentation. Figure 2 shows the results of this experiment, which confirmed that the four-wing "double-hummingbird" vehicle configuration conceived by the University of Toronto Institute for Aerospace Studies (UTIAS) is effective. In this configuration, two pairs of wings dynamically balance the vehicle and increase the amount of clap–fling thrust augmentation over that of a single pair.

The data of Fig. 2 were produced with the BIRIB-04 wing design operating at a flap amplitude of 76 deg as imposed at the wing root for both cases. Because of wing flexibility, the leading-edge spars at their tips actually flapped with an amplitude closer to 90 deg and the trailing edges of adjacent wings would touch at the extremes of the stroke. This motion was readily seen using a stroboscope. All wing designs showed the benefits of the clap–fling phenomenon to varying degrees. Figure 2 shows that, for example, the BIRIB-04 wings attained a 35% increase in the thrust-to-power ratio, on average, when clap flinging. Some wing designs gave as much as a 50% increase in thrust and a 40% increase in thrust-to-power ratio when clap flinging. While all wings showed these benefits of clap–fling operation, it should also be made clear that no effort was made to optimize wings to operate in isolation (not clap flinging). In all comparisons between the clap–fling case and non–clap–fling case, the flapping amplitude was kept constant.

Additional insight into the clap–fling phenomenon was gained through flow visualization using both tufts and a hot wire anemometer, as performed by El Khatib [11]. This experiment showed a beneficial flow-straightening property of the UTIAS double-hummingbird clap–fling design. It was found that the symmetric nature of the design caused flow that would otherwise have gone in a nonthrust direction to be deflected in the thrust direction.

Another important result from these bench tests was how the thrust/power ratio (T/P) of the clap–fling designs compared with lifting-rotor performance. Figure 3 shows a summary of these results for the best-performing wings after the first two years of the program (identified as BIRIB-04, BIRIB-07, and BAT-12). In all cases, data were taken on the previously discussed test rig and used a 75% motor efficiency and 90% drive-train efficiency. Note that in Fig. 3, the hovering performance is compared using the thrust-to-power ratio and not the figure of merit as is common with full-sized rotorcraft. The definition for figure of merit depends on induced velocity, which disguises the fact that it depends on thrust and disk area. Vehicles with higher disk loadings (wing loadings) have artificially higher figures of merit than do vehicles with a lighter disk loading. For this reason, thrust-to-power ratios are quoted along with their disk loading—and valid comparisons made only between vehicles with

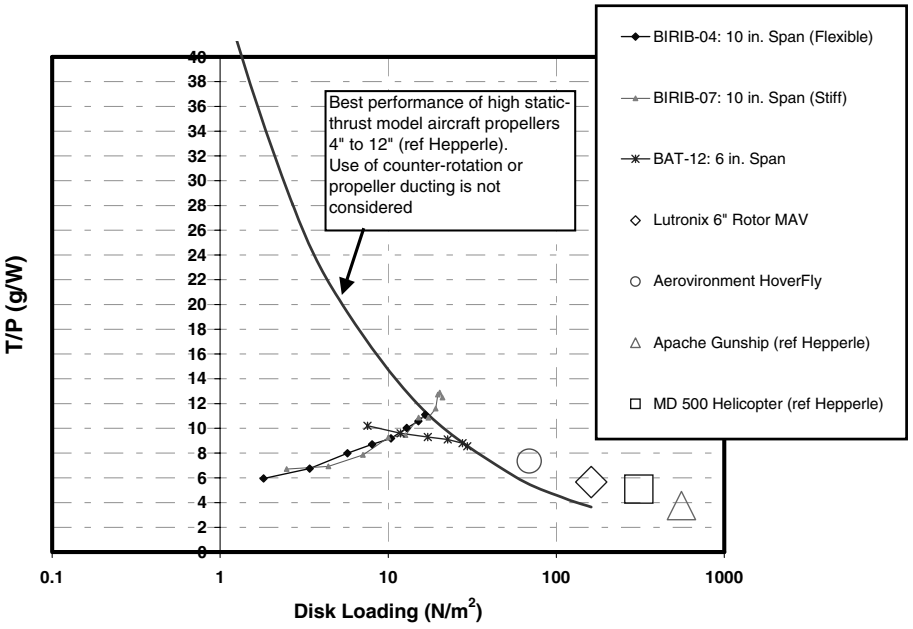

Fig. 3 Hovering performance of flapping wings compared to rotorcraft.

similar disk loadings. The solid line represents the hover performance of propellers or rotors in the Reynolds number regime of 50,000–200,000. The reference curve for the best high static-thrust producing model aircraft propellers was extracted from Hepperle's work on small propellers[‡‡] and the solid data points represent the flapping-wing configurations tested at UTIAS. It is seen that these can match the theoretical T/P of high-thrust rotors. Also, the behaviors of example rotorcraft, both MAV scale and full scale, are co-plotted. This developmental work is described in greater detail by Bilyk [12].

It must be pointed out that the wings are built "flat," with no camber or twist. Camber is provided, in the course of flapping, by aeroelastic response to the cyclic aerodynamic and inertial-reaction loads. Therefore, it was important to build in the correct amount of compliance to the wing's structure for best performance (described later).

The development of the wings was primarily experimental, taking advantage of the fact that the wings could be quickly made and tested. During the first two years of the project, as described in [12], a body of experience was established that enabled a rapid convergence toward effective designs. Manipulations of stiffness were found to be far more fruitful than were planform variations and so were investigated more thoroughly. Leading-edge spar stiffness was set at a value such that at the specified flapping-actuation angle, adjacent leading edges would come close, but not touch, at the extremes of the stroke. If leading-edge spars did touch, this absorbed considerable additional power and produced additional noise with no gain in thrust. Rib stiffness was altered to produce more deflection at the tips where wing speed was greatest.

The BAT-12 series of wings represented the pinnacle of 6 in.-span wing development both in terms of thrust-to-power ratio, ease of fabrication, and robustness. A BAT-12 wing is shown in Fig. 4, and these are all constructed with a PEEK (polyetheretherketone) skeleton and Mylar membrane. The skeleton is covered on both sides with Mylar skin using spray glue as the adhesive. Each BAT-12 wing had a mass of less than 0.25 g. Note that the airfoil is essentially a flat plate with a leading-edge thickness at the main spar of about 0.5 mm and a very thin trailing edge consisting of only the Mylar membrane material. The BAT-12 wing design, and its later derivatives such as the 14 in. span Webwing series, was well suited to systematic

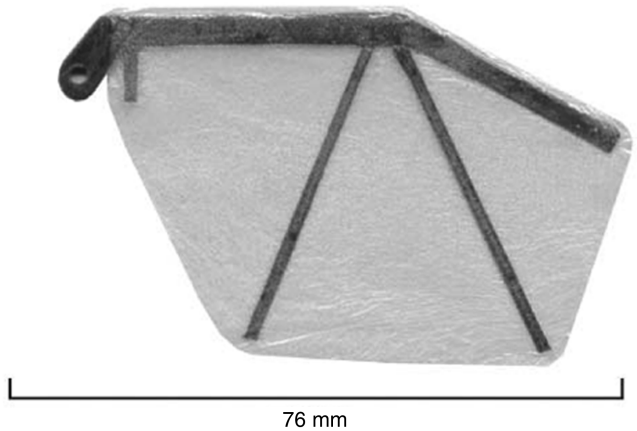

Fig. 4 BAT-12 wing showing heat bonded PEEK skeleton and Mylar skin.

variation of stiffness properties by altering the thickness (number of layers) of carbon and/or PEEK in the spar and ribs.

The BIRIB family of wings was similar to the BAT-12 wing in that they had a main leading-edge spar, but differed in rib geometry as shown in Fig. 5. The main spar and the ribs were made from commercially available carbon fiber rods of circular cross section.

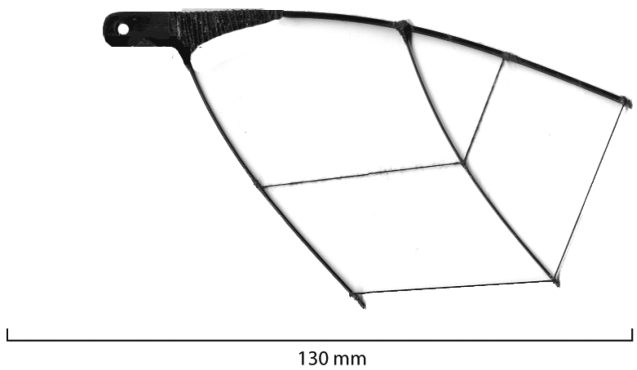

Fig. 5 BIRIB-04 skeleton structure. Leading-edge spar diameter = 0.7 mm.

[‡‡]Data available online at http://www.mh-aerotools.de [retrieved 3 May 2007].

Table 1 Summary of selected wing-design details

Wing designation	Semispan (from flap axis)	Maximum chord	Leading-edge spar notes
BAT-12	76 mm	43 mm	0.6 mm thick × 3.2 mm chord at root, 0.35 mm thick × 2.25 mm chord at tip, PEEK
BIRIB-04	130 mm	62 mm	0.7 mm diam carbon rod
BIRIB-05	130 mm	62 mm	1.0 mm diam carbon rod
BIRIB-06	130 mm	62 mm	1.25 mm diam carbon rod
WEBWING (SF-2.5)	180 mm	88 mm	1.4 mm thick × 3.35 mm chord at root, 1.0 mm thick × 3.1 mm chord at tip, carbon fiber
WEBWING (SF-3)	180 mm	88 mm	1.1 mm thick × 3.25 mm chord at root, 0.85 mm thick × 3.1 mm chord at tip, carbon fiber

Before being covered on both sides with Mylar skin, the ribs were preflexed to their desired position using polyester thread. Selected details of some of the different wing designs are summarized in Table 1.

Thrust production and power usage as a function of flapping frequency were measured on the test rig for the BAT and BIRIB series of wings, and a sample of this data for the BAT-12 is given in Fig. 6.

It must be emphasized that these clap–fling wings do not represent the most energy-efficient designs possible. The intention was to obtain high thrust within a limited actuator area (area swept by the wings). In nature, one of the largest animals to use the clap–fling action is a pigeon. In this case, the purpose is to take off rapidly in an "escape" mode, which gives rise to the loud characteristic wing-banging noise. However, the energetics is such that this can only be sustained for a limited amount of time. In a way, this is nature's afterburner. However, for MAV application, this holds the promise for a small hovering vehicle with a useful payload capability.

All wings built in the first three years, including the BAT and BIRIB series, were constructed by hand in a labor-intensive process,

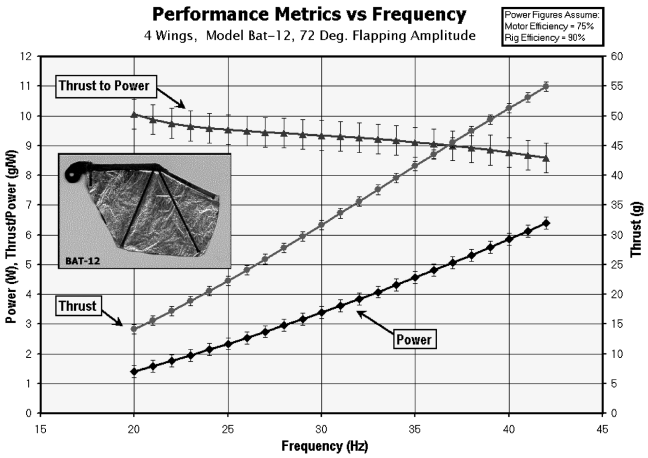

Fig. 6 Thrust-to-power ratio for BAT-12 wing set as a function of frequency.

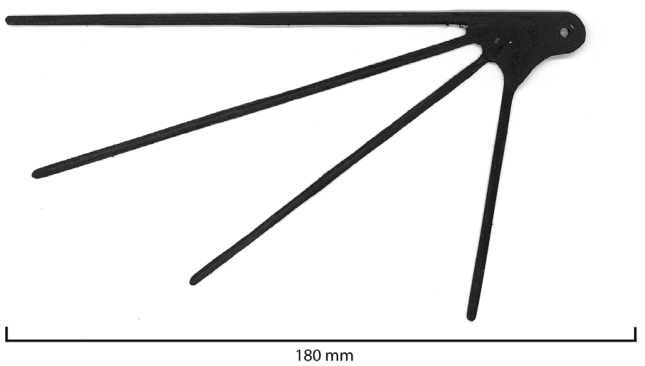

Fig. 7 Wing framework of the Webwing design as used on SF-3.

and there remained some question as to the repeatability and consistency of their construction. In the final year of the program, a different method of wing construction with "prepreg" carbon fiber was used for the SF-2.5 and SF-3 vehicles. This type of carbon fiber is manufactured with an appropriate amount of epoxy premixed into the fiber; hence is it not only convenient to use but also has remarkable consistency in application. These benefits were the prime reason for switching from the previously used "PEEK" material, which consists of unidirectional carbon fibers embedded in a thermoplastic polyetheretherketone matrix.

To produce a wing, the prepreg fiber is cut into strips of various lengths, and then arranged in layers on a flat surface to create the wing pattern and elastic properties for the desired twist and camber during flapping. When the arrangement of these strips is complete, heat and pressure are applied simultaneously to join the carbon fiber strips and cure the epoxy within the material. Because the epoxy cure temperature is 250°F, a temperature-controlled oven was constructed. A vacuum pump was used to apply pressure, allowing for a uniform application of approximately 13 psi. The vacuum-bagged parts are placed within the curing oven for approximately 2 h. This is a well-established method of processing composite materials. After this step, all that remains is to shape the wing roots for attachment to the wing hub. An example of the resulting wing framework is shown in Fig. 7. This framework is sandwiched between two layers of 1 mil Mylar to give the final wing.

Experiments were performed with different wing-design patterns, the main variation being the number of layers of strips. This controls the relative stiffness of the wing spars which, in turn, plays a crucial role in wing performance. Overall wing stiffness was also greatly influenced by the manner of attachment of the Mylar skin. By including a degree of slackness in the skin, especially at the wing root, the torsional stiffness was made very nonlinear. This allowed the wing's torsional stiffness to be very low at light loadings, but to rise sharply as loading increased and the stiffness of the carbon skeleton dominated. After a few preliminary trials to gain experience with this type of construction, four wing-layout patterns were tested. Each was subjected to a series of design iterations, at the end of which an entire set of wings in each pattern was produced. These were tested on SF-2.5 (a fuel-powered free-flying vehicle, described later) to determine relative and absolute performance. A design named "Webwing," which produced a satisfactory thrust margin, was selected as the final wing design. This is shown in Fig. 7 (and mounted on the Mentor vehicle in Fig. 13b).

III. Unsteady-Airfoil Analysis

In parallel with the experimental wing development work, Zdunich [13] developed a 2-D model of the aerodynamics over a section of a flapping wing. This was a time-marching, discrete-vortex analysis, with imposed Kutta conditions at the leading and trailing edges; and it was shown to effectively model leading-edge and wake effects in both hover and forward flight. A measure of translational flapping-wing flight is the advance ratio, defined by $\lambda = Vc/(2f)$, where V is the flight velocity, c is the airfoil's chord, and f is the flapping frequency in Hz. It was found that at high advance ratios, as experienced in fast translational flapping flight, attached flow is guaranteed and the trailing-edge Kutta condition sufficed. However,

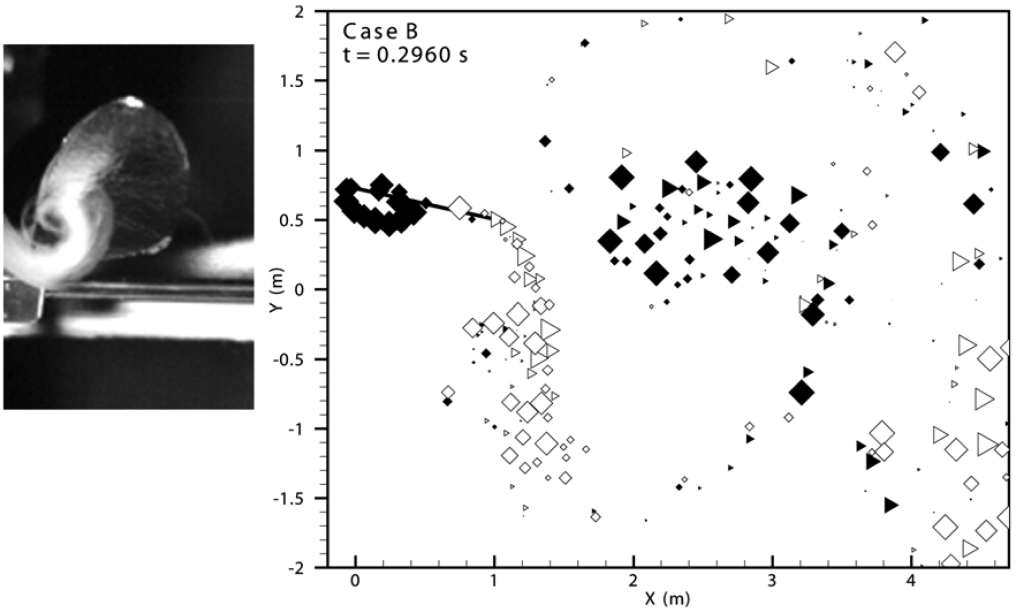

Fig. 8 Flow visualization comparison between experimental (left) and theoretical results (right).

as the advance ratio decreases, approaching and including hovering conditions, a viable solution required the imposition of a Kutta condition on the leading edge, giving vortical shed wakes from both the leading and trailing edges as seen in Fig. 8. This matches the experimental observations obtained with smoke and high-speed video (also shown, at left, in Fig. 8).

The general methodology is presented here: bound vorticity was modeled using discrete vortices arrayed along the chord line with tangential flow conditions prescribed at associated control points. Two different unsteady Kutta conditions were developed. One prescribed zero pressure difference across the chord line at the leading and trailing edges and yielded nonlinear equations. The other simply prescribed tangential flow at these points and gave a linear system of equations. A comparison of these two Kutta conditions with the well-known Wagner function showed similar results between the two different ways of imposing the Kutta conditions, and so the linear system was favored due to a faster and more robust solution. The final boundary condition was the conservation of vorticity, in which the change in bound vorticity between time steps is shed into the wake as discrete-vortex elements that are free to move with the net velocity at their centers. The model generates instantaneous force and moment coefficients using the unsteady pressure (unsteady Bernoulli) equation. A representative sample of this data is included as Fig. 9.

One extensively documented case in which large-scale separated flow exists is that of a blunt object in normal flow producing the vortex street. This is well suited as a test case because a flat plate airfoil may be held fixed in a steady crossflow such that vortex shedding from the leading and trailing edges results. The

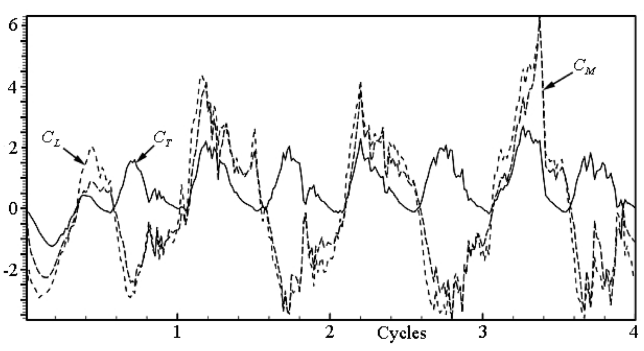

Fig. 9 Instantaneous force and moment-coefficient results.

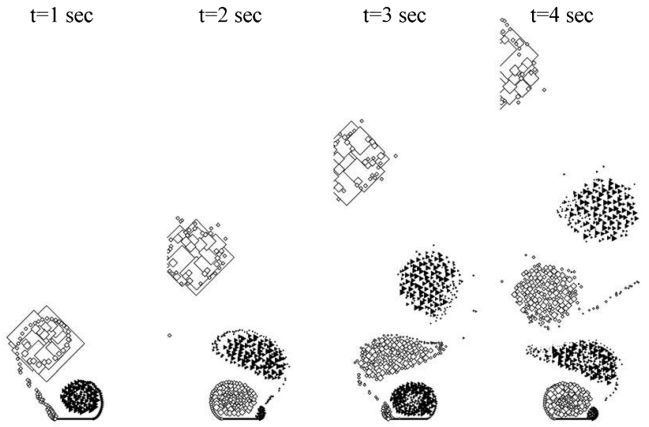

Fig. 10 Model's visualization of oscillatory wake from a flat plate in crossflow (shown at different times).

characteristic wake developed by running the model for this case is shown in Fig. 10. The Strouhal number for this test case was $St = 0.18$. Among others, Roshko's [14] experimental result for the Strouhal number associated with vortex shedding from a circular cylinder is $St \approx 0.2$. In addition, the model gave an average drag coefficient of $C_D = 1.82$ while Hoerner [15] gives an expected value of $C_D = 1.98$. Note that the model was not manipulated to get better agreement for this test case. This gives confidence that this inviscid model captures the important flow structure and the large-scale features that dominate the force production of a thin airfoil in low-Reynolds number viscous flow. That is, the excellent agreement of both Strouhal number and force coefficient show that the model is well suited to the flow structures caused by a very thin airfoil operating at low advance ratios, where large-scale flow separation exists. It is important to note that these results have been obtained from an inviscid-flow solution, with the viscous effects simulated by the imposed Kutta conditions. This simplification affords a great ease and speed of calculation compared with a Navier–Stokes solution, and therefore the model could be readily used as a tool to support the wing-design effort. This model did provide guidance, but time did not permit the development of this analysis to the two-airfoil clap–fling case or extensions to finite spans. Any further development of the Mentor would be well served by such an enhancement.

It should be mentioned that a similar inviscid time-marching analysis has been independently developed by Ansari et al. [8]

where the key difference is the use of conformal transformations, with most calculations performed in the circle plane. Also, the model was used in a blade-element analysis for a quasi-3-D study of finite wings.

IV. Drive Mechanism Development

Just as the flapping-wing aerodynamic propulsion system was inspired by natural flyers, the flapping-wing actuation system was also intended to copy the capabilities of natural flyers by using an actuator that emulated natural muscle. Electroactive polymer artificial muscles were to be the basis of a lightweight, quiet, and simple flapping-wing propulsion system.

EPAM actuators are based on the deformation of a thin elastomeric polymer due to the electrostatic stresses imposed by compliant electrodes on both surfaces. These stresses are commonly referred to as Maxwell's stress. EPAM actuators, also known in the literature as "dielectric elastomers," are capable of large strain deformation with fast response speed and good efficiency (Kornbluh et al. [16]). The ability to replicate the strain and forces of natural muscle is why the technology is often referred to as "artificial muscle." Several elastomeric polymers can form the basis of EPAM actuators. The two most promising polymers investigated in this project were based on commercially available silicones and acrylics.

Several biologically inspired flapping mechanisms based on electroactive polymer artificial muscles were demonstrated at SRI. Figure 11 shows an example of an insect-inspired flapping-wing mechanism. The entire assembly has no bearings or sliding parts. It includes "living hinges" made of thin stainless steel, and the linkage structure was designed to allow several EPAM actuators to be stacked in parallel to achieve greater force capabilities. This mechanism was able to produce about 40 deg of motion at 9 Hz with nine silicone actuator layers.

During the project, improvements were made to EPAM actuator designs, manufacturing techniques, and materials. However, limitations in scaling up the muscles to the power levels required for vehicles weighing about 454 g (1 lb, like the current flyers), as well as the nonavailability of batteries and microelectronics that can efficiently deliver the high voltage needed to drive the muscles, led to the use of more conventional (albeit also high performance) actuators such as rare-Earth magnet brushless dc motors. Figure 12 shows the drive mechanism used to convert the high rotational speeds of the motor to the lower-frequency flapping of the wings as implemented on the electric Mentor (SF-3).

The drive mechanism was constructed from a combination of custom parts and commercially available gears, bearings and shafts, though the gears were further lightened by thinning and drilling. The

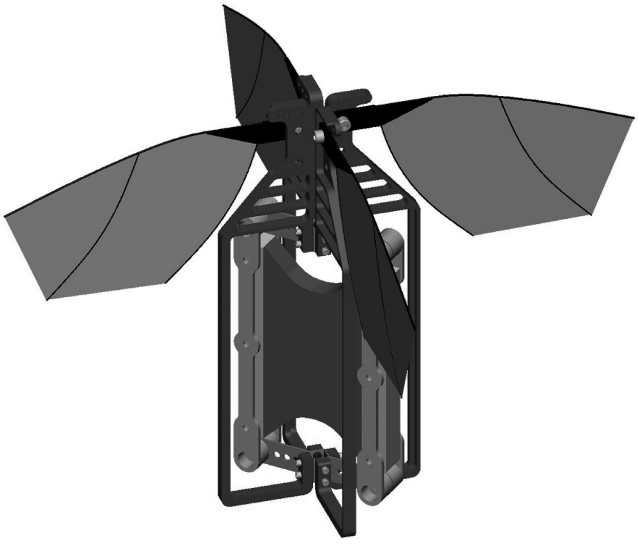

Fig. 11 T-flex mechanism: insect-inspired flapping-wing mechanism that uses a stack of EPAM actuators attached to a flexible linkage.

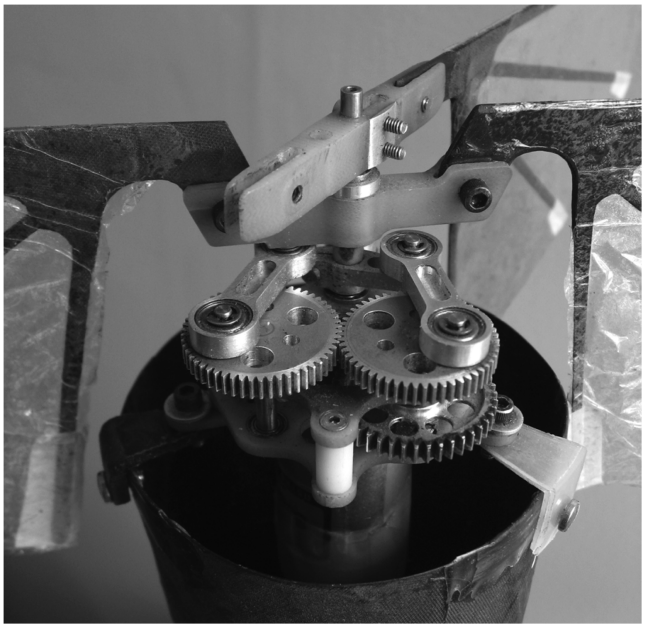

Fig. 12 Drive-reduction mechanism of SF-3 vehicle (nearest wing removed for clarity).

wing-flapping mechanism consisted of a multistage gear reduction coupled to a symmetrical pair of four-bar linkages. These linkages drove a set of nested concentric tubular shafts to which were attached the four wings, with two wings per shaft attached diametrically opposite to one another. Note also that the wings were actuated with only a single degree of freedom. This was made possible by the highly compliant aeroelastically tailored wings and eliminated the need for very complex and potentially fragile, and heavy, actuation methods.

It was also recognized that EPAM could address a technical need in the area of fast and lightweight control surface actuators. Existing COTS (commercial off the shelf) approaches are often not viable for actuation in very small vehicles. For example, alternative actuation schemes involving piezoelectric materials are currently too heavy and have small excursions, and shape memory alloys are too inefficient and have inadequate frequency response. Because the power levels associated with EPAM-based control-surface actuators are lower than those of the actuators required for flapping the wings, these control surface actuators might be realized before EPAM technology evolves for direct wing flapping. Several unimorph bending-beam actuators that use EPAM were demonstrated. It should be noted that other small air vehicles (not just flapping wing) could also benefit from this actuator development. SRI also demonstrated several configurations that could be used for lightweight, simple, and compact actuators for flow control, and these may offer advantages over piezoelectric and electromagnetic actuators currently being used for such applications.

In any event, as mentioned previously, the demonstration vehicles did not incorporate EPAM technology and were powered by internal combustion (IC) and electric power.

V. Flight-Demonstration Models

The first demonstration model, named SF-2.5 and shown in Fig. 1, incorporated a set of four flapping wings actuated in the horizontal plane (when in hovering orientation). The first sustained, stable, and controlled flights of this vehicle occurred in March 2002. As discussed previously, SF-2.5 makes use of the clap–fling mechanism to augment the thrust. The hub of the flapping wings is located about 4.5 in. above the vehicle's center of gravity, and the wings (of 14 in. span) are actuated at a nominal frequency of 30 Hz by a 0.074 $in.^3$ internal-combustion engine (manufactured by the Norvel Company for small model helicopters). This drives a gear-reduction mechanism followed by a rotary-to-oscillatory linkage. When fully

fueled, the vehicle weighed 580 g. Thrust production was controlled by altering motor speed, which is directly linked to flapping frequency. By reducing or increasing flapping frequency by just a few hertz, the vehicle could be made to climb or descend quite rapidly. Motor speed was the only input directly controlled by the human operator (not influenced by the onboard computer) and therefore, as seen in videos of the flights, is the most erratic. A control loop could be closed on throttle, but was not done for this development program.

SF-2.5 was controlled with four independently actuated fins of approximately the same size as the flapping wings. Control surfaces for both SF-2.5 and SF-3 were flat plate wings, hinged to actuate at the quarter chord. These fins had, at different times, rectangular, round, and sharp leading and trailing edges. Differences of this kind had little influence on their effectiveness because the onboard computer automatically compensated by changing the actuation angle. The control fins had, on average, a semispan of 14 cm and chord of 11 cm, and were located about 4.5 in. below the center of gravity of the vehicle and controlled by an onboard programmable logic board that was custom configured for this application by Xiphos Technologies (Montreal, Canada). The controller board takes commands from the pilot relating to intended vehicle rotation rates and compares them with the outputs of 3-axis rate gyros. Together, these data serve as the necessary input and feedback in a 3-axis proportional–integral–differential (PID) control system. The result is that the vehicle was stable in hover with no pilot input.

Following the experimental verification of gain coefficients estimated by the simulation, discussed in the next section, the SF-2.5 was evaluated in hovering flight and was found to be stable and controllable. Hovering flights of more than 1 min were achieved (the vehicle carries fuel for up to 6 min of hovering flight). The vehicle was even more controllable while climbing than in the hovering orientation because of the increased flow speed over the fins. Therefore, it was necessary to exercise more care while descending because the vehicle's descent rate could be similar to the speed of the downwash from the flapping wings. As a result, the authority of the control fins could be greatly reduced if the vehicle descended too quickly.

After the hovering-stability experiments, translational flight experiments began. It was initially decided to concentrate on very slow-speed translation by pitching the vehicle slightly out of the hovering orientation while in hovering flight. An effect not predicted by the simulation was the vehicle's ability to pitch over as much as approximately 10 deg from vertical without any perceptible lateral or vertical acceleration. It was surmised that a balance of forces was being created laterally between the thrust force of the wings and the lifting forces of the control fins in the wing's downwash. At attitudes in excess of 10 deg from vertical, the vehicle would begin to translate laterally. It was found that the vehicle could easily be accelerated to approximately walking speed (3 m/s). This speed would be maintained if the vehicle's attitude remained about 15 deg from vertical. At higher pitch angles from vertical, the vehicle would become unstable.

The hovering experiments with the SF-2.5 vehicle showed it to have a thrust capability significantly in excess of the vehicle weight. It was also noted that the vehicle was quite stable while ascending. Therefore, it was decided that the best method of attempting a transition from vertically oriented hovering flight to horizontally oriented high-speed translational flight would be to accelerate the vehicle upward and then gradually pitch it into a horizontal position.

The vehicle flight simulation stated that the PID control coefficients necessary for stable hovering flight are different from those required for stable high-speed translational flight. A smooth decrease in control coefficients would be required as the vehicle accelerated; however, as configured, the Xiphos control board could not alter the control coefficients during flight. If one were to attempt high-speed flight using the PID coefficients appropriate to hover, the vehicle would become unstable at approximately 11 m/s.

Nonetheless, some insights were obtained into the fast forward-flight regime. On several occasions, when exploring the vehicle's hovering flight performance, the vehicle's throttle was applied too aggressively while the vehicle was inclined from vertical. On those occasions the vehicle entered a high-speed translational flight mode for a brief period (less than 3 s) until it reached the speed at which the PID coefficients were inappropriate and a tumble occurred, just as predicted by the simulation. Because of the vehicle's rapid motion, small size, and symmetry, it was not possible for the pilot to determine its attitude.

Because quiet operation is important in a close-range reconnaissance vehicle, an electric-powered version was also built (Fig. 13). This vehicle, representing the culmination of the technical effort during the project, could hover controllably for periods that were limited in duration by the low-energy density of rechargeable batteries. The electric-powered version was shown to be capable of higher-speed cruising flight (estimated up to 35 kph). Cruising flight was demonstrated by outfitting the vehicle with a larger set of tail fins that allowed for stable horizontal flight. The ability to controllably transition from cruising to hovering flight modes was not demonstrated.

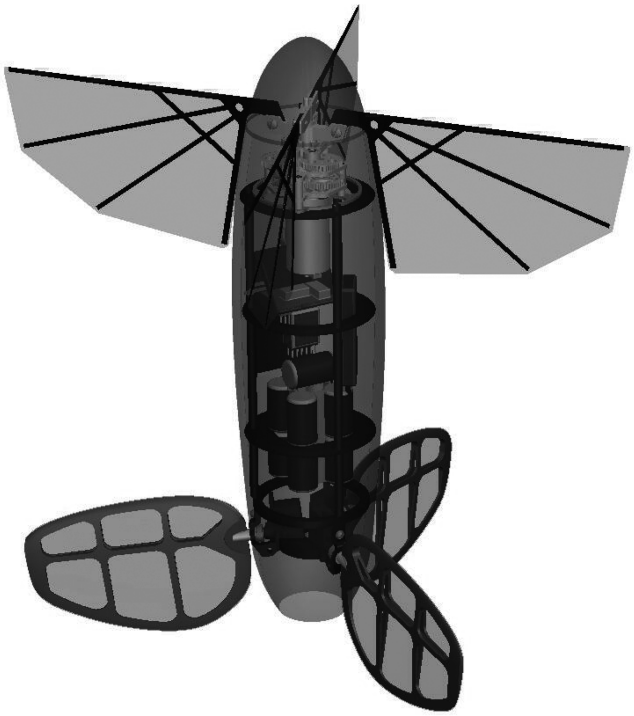

a)

b)

Fig. 13 a) Transparent computer model of electric-powered demonstration vehicle (SF-3). b) Electric-powered demonstration vehicle (SF-3).

Table 2 Selected vehicle parameters

	SF-2.5 (IC powered Mentor)	SF-3 (electric-powered Mentor)
Maximum span	14 in. (0.36 m)	14 in. (0.36 m)
Mass	580 g	440 g
Nominal flapping frequency	30 Hz	30 Hz
Engine/motor and rated power output	Norvel 0.074 $in.^3$ model helicopter glow engine	Astroflight 020 brushless motor with sensor feedback motor controller
Gear reduction	11.3:1	12.32:1
Power source and quantity	Nitromethane (51 ml)	NiCd battery pack (8 cells, 600 mAh each)

Table 3 Component mass breakdown of both internal combustion (SF-2.5) and electric (SF-3) Mentor vehicles

Component	SF-2.5 (IC powered Mentor)	SF-3 (electric-powered Mentor)
Wings (total mass)	14 g	11 g
Drive mechanism (from motor shaft output to wing attachment points)	108 g	44 g
Fuselage structure	75 g	40 g
Control servos	30 g	24 g
Control fins	53 g (incl. dead weight for balance)	12 g
Onboard control system	40 g	40 g
Radio receiver	10 g	10 g
Motor	116 g (incl. muffler, clutch and pinion)	105 g (incl. motor, motor controller, flywheel and pinion)
Fuel tank empty	17 g	N/A
Fuel	55 g	N/A
Primary battery	N/A	154 g
Control-system battery	48 g	N/A
Other (fasteners, wire, etc.)	14 g	N/A
Total	580 g	440 g

SF-3 was powered by a brushless electric motor (Astroflight 020 with sensor feedback motor controller) driving a gearbox and rotary-to-oscillatory transmission. The energy to drive the motor was supplied by a battery pack of 8×600 mAh NiCd cells. The total vehicle weight was approximately 440 g, which is less than the nearly 580 g of the fully fueled SF-2.5. The wing design for SF-3 was virtually identical to the more robust wings used for SF-2.5, except that the stiffness was reduced for greater efficiency at the lower thrust required for hovering. The flapping frequency was approximately 30 Hz. As with SF-2.5, the SF-3 vehicle was controlled by a 3-axis PID system using 3-axis gyros for feedback and taking angular-rate commands from a pilot via radio control. The selection of the electric motor and gear-reduction ratio was aided by extensive dynamometer testing. COTS batteries were tested with SRI's battery testing facility, and NiCd batteries were selected over NiMH based on measured duration at the required power output. Small COTS servos were tested with a specially constructed apparatus that allowed the selection of the fastest and lightest units.

Before electric-vehicle hovering tests began, the simulator was used to determine appropriate control-system gain coefficients. Once again, the simulation pointed to gain coefficients close to the eventual flight-tested optimums, illustrating the consistent performance of this useful tool. With gains thusly determined and input, SF-3 hovered stably on its first flight. The vehicle was very well stabilized in attitude, and throttle control was much easier than on the IC vehicle because of a reduced lag in motor control. Unfortunately, flight times were severely restricted by the limitations of the batteries. Although the batteries contain enough energy to fly for over 1.5 min, they do not have the ability to discharge power this quickly. As a result, continuous hovering flights rarely exceeded 20 s before the power output of the batteries began to decline. After allowing the batteries a few moments to "refresh" themselves, a second or even third 20 s flight was possible.

Although such short-duration flights would appear to suggest that battery-powered flight is not practical, it must be recognized that the NiCd batteries were selected because they offered the needed current delivery and not because they have particularly high-energy density. If the mass of the vehicle was slightly reduced, then NiMH batteries, having 4 times the energy density, could be used. Further increases in flight duration, allowing hovering times of several minutes (similar to that for the fuel-powered version) could be achieved by using specially designed lithium polymer primary batteries. Because of cost at the time, such batteries were not evaluated during the project.

Long distance forward-flight attempts were not made with the SF-3 vehicle due to the PID coefficient issue described previously. However, in the few instances where SF-3 was unintentionally overaccelerated, the vehicle flew briefly in translation without loss of altitude before hitting the walls (where it suffered minor damage to the wings and fins). These brief flights were very encouraging with respect to the future capability for high-speed translational flight (not to mention the demonstrated relative ruggedness of the vehicle). Vehicle parameters of interest are listed in Table 2 and a component mass breakdown is given in Table 3.

VI. Stability and Control

The flight-dynamic simulation, developed by SRI, is capable of real-time operation and permits pilot-in-the-loop studies of flight maneuvering, evaluations of various stability and control-augmentation strategies, and evaluations of vehicle configurations. The model's output includes real-time aircraft state data as well as time-history graphs. Stability derivatives are extracted automatically from the real-time model. The model can also be run in a batch mode, permitting the time-history analysis of the vehicle's response to repeatable control inputs (doublets). Figure 14 illustrates the significant elements of the program and their interactions, and Fig. 15 shows a side-by-side comparison of the operation of the simulation and the SF-2.5 flapping-wing vehicle.

The simulation display is at the upper left and the actual flapping-wing vehicle in hovering flight is at the upper right. The lower left shows the pilot using the simulation via a joystick controller, and the lower right shows the pilot operating a modified, single stick radio controller for the actual vehicle.

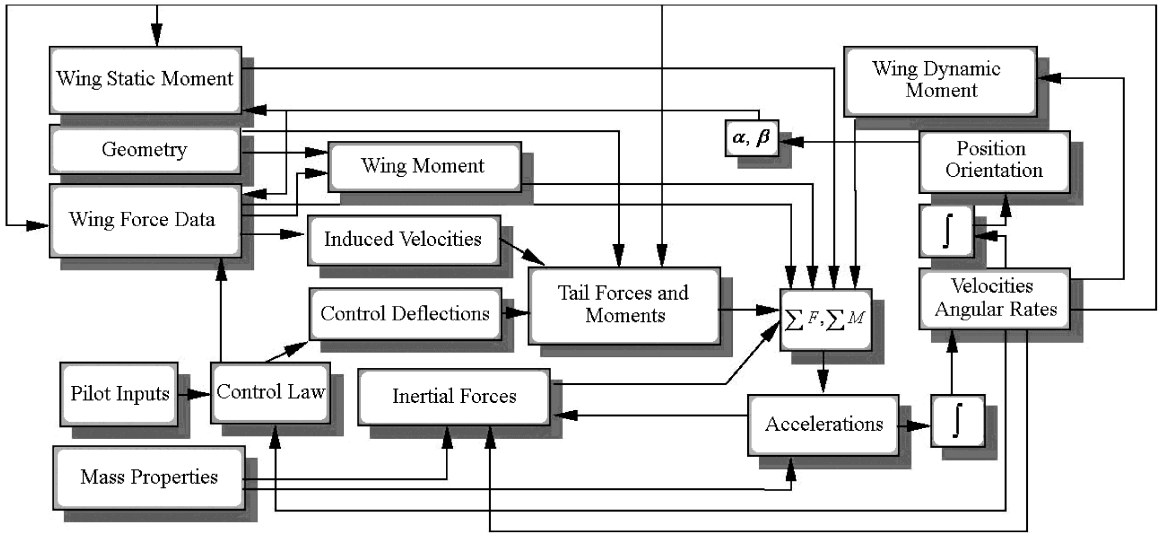

Fig. 14 Structure of program for dynamic modeling of Mentor vehicle.

Fig. 15 Flight simulation (left) and actual flying vehicle (right).

The dynamic model is based on wind-tunnel measurements made with the flapping-wing system in a UTIAS low-speed tunnel, as described by MacMaster [17]. Total force and moment components for the flapping-wing system were tabulated as functions of flight velocity (expressed as nondimensional advance ratios) and the direction of flight (characterized by the angle between the flight-path vector and the aircraft's longitudinal axis). Example results are shown in Fig. 16. Also, these data were measured through the full range of achievable flight conditions. Induced velocities were predicted from momentum theory and measured thrust performance. Forces and moments generated by control surfaces were predicted based on influences from vehicle translation, induced velocities, body rotations, and control surface deflections. The stability-augmentation system was modeled as a PID controller, based on attitude and angular-rate data from the prior simulation time step. Servo actuator response was modeled based on measured performance. The dynamic model permits rapid iteration of aerodynamic configuration, center of mass, and control gains in both piloted and batch modes of operation.

One result of this work was that the vehicle was purposely made neutrally stable as a compromise between stability in the hover mode and stability in the forward-flight mode. In forward flight, when the vehicle is pitched over and flying much like a conventional aircraft, static stability is provided in the usual way: by placing the center of mass ahead of the neutral point. In a hover, it was found that the opposite arrangement gave static stability. Increasing the stability to favor either of the flight modes was to the detriment of the stability in the other. Therefore, the vehicle was made neutrally stable and was actively stabilized by the onboard control system. In this way, the computer could more easily stabilize the vehicle in either flight mode because it was not fighting a strong unstable tendency in one of the flight modes. This strategy was proven to work when, on one test, the pilot unintentionally increased the flapping frequency too rapidly and the vehicle quickly rose, pitched over nearly parallel with the ground, and continued to fly stably and without altitude loss for several meters. Flight beyond this speed would have necessitated the scaling of control gains, which was not implemented.

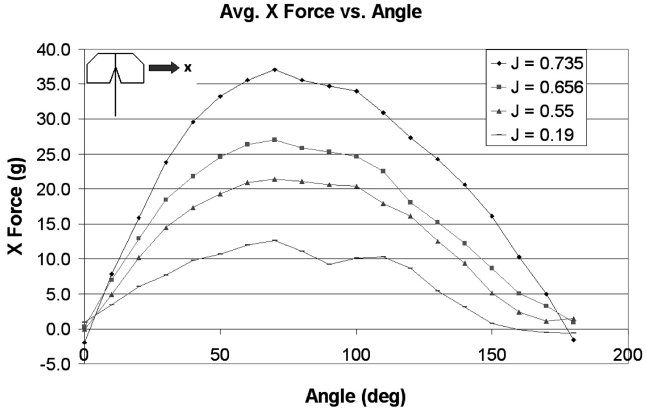

Fig. 16 Example of wind-tunnel force data used for simulation inputs (J = advance ratio).

VII. Concluding Remarks

A. Accomplishments

Project Mentor, a partnership between SRI and UTIAS, sought to develop a flapping-wing lift/propulsion system that would demonstrate performance advantages over current technologies such as motor-driven propellers, rotors, or jets, for MAV application. The project focused on the hovering and slow-speed flight regime for two reasons. First, this regime presents a greater challenge to the vehicle's performance than translational flight, especially as compared with propeller-driven aircraft. Second, and more important, the regime encompasses a great number of the possible missions for small flyers. Work during the first three years of the contract focused on experiments to better map out the wing design and operational parameter space, as well as the development of analytical tools that would enable the quick evaluation of new wing designs and operating conditions (e.g., flapping frequency, root

flapping angle, etc.). One of the most useful tools was a flight-dynamic simulation that was developed to enable the evaluation of vehicle stability and guide the design of the optimal vehicle configuration. As a result of this technological foundation, two demonstration flight vehicles were made that performed successful hovering and slow translational flight. A great deal was learned from this, pertaining to the practical operation of such unique aircraft. These tests also elucidated future developmental directions.

B. Feasibility of Flapping Wings for MAVs

A hummingbird can cross the Gulf of Mexico without eating, swoop from a tree top, and hover in front of a flower. Inspired by the amazing flight capabilities of numerous creatures found in nature, flapping-wing propulsion promises to offer a combination of capabilities that are not currently available in conventional rotor or propeller-driven vehicles. This inspiration was the key motivation for undertaking the project. However, a small flying vehicle that could actually realize the full benefits of flapping-wing flight was beyond the current state of the art. The realization of such a vehicle requires advancements in configuration, wing design and aerodynamics of flapping, and especially propulsion-system design. In the course of this research, the promise of these potential advantages was demonstrated and is summarized below.

1. Efficiency at High Disk Loadings, for High Payload Capability and Gust Resistance

The Mentor flapping-wing vehicle has shown aerodynamic efficiency in hovering (thrust-to-power ratio) that is already similar to that of the best rotors. This result is significant, given the early stage in the development of flapping-wing design and operation, relative to the maturity of rotors. There is certainly much opportunity for future improvement. Further, this high relative efficiency is exhibited at relatively high disk loading (the swept area of the wings, divided by the vehicle weight). This ability to hover efficiently at high loadings allows for vehicles with significant payload mass as well as vehicles that inherently offer some resistance to gusts of wind and atmospheric turbulence.

2. Multiple Flight Regimes with High Efficiency and an Economy of Design

As with a hummingbird, a flapping-wing vehicle can potentially hover and efficiently cruise. It effectively combines the advantages of an airplane and a helicopter. Vertical takeoff and landing (VTOL) vehicles that attempt to combine airplane and helicopter capabilities often require separate lift, propulsion, and control devices. In contrast to VTOL vehicles, flapping wings provide both thrust and a significant portion of the necessary lift. Additionally, the vehicle might not necessarily need to reconfigure itself to switch flight regimes. Further, it should be noted that the Mentor's wings were of very simple construction, built flat. The aeroelastic characteristics provided the required twist and camber both for hovering and for horizontal translational flight. This compares very favorably to the greater complexity of the fabrication and articulation of rotors and propellers.

3. Proven Stability in Hovering for Easy Operation and Guidance

The test vehicles have demonstrated exceptional stability in hovering flight with the use of low-cost COTS rate gyros and a simple control algorithm. An operator would need only to provide minimal control input and would not need to be highly skilled. The vehicle could also be interfaced to other sensors and systems for more autonomous navigation or obstacle avoidance.

4. Scale-Down Ability and Biomimicry for Stealth

The aerodynamic advantages of flapping-wing flight stem from small-scale phenomena in unsteady aerodynamics, which become even more important in smaller sizes such as those of insects. Because these flapping-wing vehicles are intended to operate at close range, their small size is an advantage because smaller vehicles are naturally harder to detect. As micropower systems, sensors, and electronics mature, the possibility of scaling down such vehicles and the use of flapping wings becomes more important. Also, because small flying creatures are commonly encountered, it follows that a small flyer that looks and sounds like a natural flyer would not be as noticeable. Thus, biomimicry is possible. It should be further noted that nature has evolved many flapping-wing flyers, such as owls, that make almost no sound at all.

C. Future Research Directions

In the course of this research, it was clear from the flight testing that future versions of such a vehicle must have an airspeed sensor and control coefficients that vary with flight speed, so that the coefficients can be automatically updated to ensure stable flight. Also, the vehicle must be modified in some way so that the pilot can determine the orientation while in high-speed flight. Alternatively, a more autonomous flight-control system could be used to maintain attitude and flight path.

At the high wing loadings of the Mentor vehicle, even the aerodynamic noise of the wings alone is significant. Although quiet flight was not conclusively demonstrated on this project, it is felt that flapping wings have the potential to do so at somewhat lower disk loadings. An additional factor that was not fully explored was the frequency spectrum of the observed sound. Higher-frequency sound components are very directional and could allow precise location of the vehicle, which is an undesirable effect. It is expected that a low fundamental flapping frequency of approximately 25 Hz could produce a sound that is unlikely to be noticed and hard to locate.

All project goals were successfully completed, with one exception: the ability to transition between translational flight and hover. It is believed (based in part on simulations) that a modification to the firmware in the controller board, allowing for a different set of controller gains in translational flight, will enable a Mentor-type vehicle to successfully demonstrate a repeatable ability to transition between flight regimes. The current project concluded before this modification could be made.

Finally, it should be noted that certain system-level considerations point to intriguing new directions for development. In particular, improved aerodynamic efficiency is important only insofar as it allows for vehicles with improved payload, performance, or duration. Because oscillating flapping-wing motion is different from the rotational motion for rotor craft, flapping-wing propulsion systems might be able to use a fundamentally different type of actuation. For example, it does not make sense to use a fuel-burning engine that creates reciprocating motion, converts that to rotary motion, and then converts the rotary motion back to the reciprocating motion needed for flapping-wing flight. A lighter and more efficient propulsion system might be developed that directly couples the reciprocating motion to the flapping wings. This propulsion system would also be quieter because the engine would operate at only about 25 Hz, as opposed to the 500 Hz typical of small IC engines. Human hearing perception is greatly reduced at this lower frequency.

References

[1] Grasmeyer, J. M., and Keenon, M. T., "Development of the Black Widow Micro Air Vehicle," *Fixed and Flapping Wing Aerodynamics for Micro Air Vehicle Applications*, edited by Thomas J. Mueller, Progress in Astronautics and Aeronautics, Vol. 195, AIAA, Reston, VA, 2001, pp. 519–535, Chap. 24.

[2] Barrett, R., "Development History of a New Family of Subscale, Convertible, High Performance UAVs," *Workshop on Micro Air Vehicles-Unmet Technological Requirements*, Schloss Elmau, Germany, 22–24 Sept. 2003.

[3] DeLaurier, J. D., and Harris, J. M., "A Study of Mechanical Flapping-Wing Flight," *Aeronautical Journal*, Vol. 97, No. 968, Oct. 1993, pp. 277–286.

[4] DeLaurier, J. D., "The Development and Testing of a Full-Scale Piloted Ornithopter," *Canadian Aeronautics and Space Journal*, Vol. 45, No. 2, June 1999, pp. 72–82.

[5] DeLaurier, J. D., "An Aerodynamic Model for Flapping-Wing Flight," *Aeronautical Journal*, Vol. 97, April 1993, pp. 125–130.
[6] Ellington, C. P., "The Novel Aerodynamics of Insect Flight: Applications to Micro-Air Vehicles," *Journal of Experimental Biology*, Vol. 202, Dec. 1999, pp. 3439–3448.
[7] Birch, J. M., Dickson, W. B., and Dickinson, M. H., "Force Production and Flow Structure of the Leading-Edge Vortex on Flapping Wings at High and Low Reynolds Numbers," *Journal of Experimental Biology*, Vol. 207, March 2004, pp. 1063–1072.
[8] Ansari, S. A., Zbikowski, R., and Knowles, K., "Non-Linear Unsteady Aerodynamic Model for Insect-Like Flapping Wings in the Hover. Part 1: Methodology and Analysis," *Proceedings of the Institution of Mechanical Engineers, Part G: Journal of Aerospace Engineering*, Vol. 220, No. G2, April 2006, pp. 61–83; also Non-Linear Unsteady Aerodynamic Model for Insect-Like Flapping Wings in the Hover. Part 2: Implementation and Validation," *Proceedings of the Institution of Mechanical Engineers, Part G: Journal of Aerospace Engineering*, Vol. 220, No. G3, June 2006, pp. 169–186.
[9] Weis-Fogh, T., "Unusual Mechanisms for the Generation of Lift in Flying Animals," *Scientific American*, Vol. 233, No. 5, 1975, pp. 80–87.
[10] Kuethe, A. M., and Chow, C.-Y., "Chapter 4: Irrotational Incompressible Flow About Two-Dimensional Bodies," *Foundations of Aerodynamics*, 5th ed., Wiley, New York, 1998, p. 108.
[11] El Khatib, J., "Flow Visualization for a Micro Air Vehicle," M.Sc. Thesis, University of Toronto, Toronto, Ontario, Canada, 2000.
[12] Bilyk, D., "The Development of Flapping Wings for a Hovering Micro Air Vehicle," M.Sc. Thesis, University of Toronto, Toronto, Ontario, Canada, 2000.
[13] Zdunich, P., "A Discrete Vortex Model of Unsteady Separated Flow About a Thin Airfoil for Application to Hovering Flapping-Wing Flight," M.Sc. Thesis, University of Toronto, Toronto, Ontario, Canada, 2002.
[14] Roshko, A., "On the Development of Turbulent Wakes from Vortex Streets," NACA Rept. 1191, 1954.
[15] Hoerner, S., "Pressure Drag," *Fluid Dynamic Drag*, Hoerner Fluid Dynamics, Brick Town, NJ, 1965, pp. 3–17.
[16] Kornbluh, R., Pelrine, R., Pei, Q., Rosenthal, M., Stanford, S., Bonwit, N., Heydt, R., Prahlad, H., and Shastri, S., "Application of Dielectric Elastomer EAP Actuators," *Electroactive Polymer (EAP) Actuators as Artificial Muscles: Reality, Potential, and Challenges*, 2nd ed., edited by Y. Bar-Cohen, SPIE Press, Bellingham, WA, 2004, Chap. 16, pp. 529–589.
[17] MacMaster, M., "Stability of a Flapping-Wing MAV," M. Sc. Thesis, University of Toronto, Toronto, Ontario, Canada, 2001.